Inclusions on Fluid Membranes Anchored to Elastic Media

M. S. Turner*# and P. Sens§

*Department of Physics, Warwick University, Coventry, CV4 7AL United Kingdom; #Center for Studies in Physics and Biology, Rockefeller University, New York, New York 10021 USA; and §Institut Charles Sadron, 67083 Strasbourg, France

ABSTRACT   We model theoretically the effect of localized forces on a fluid membrane anchored to a uniform elastic medium. We use this as a simple model for the plasma membrane of a cell. The atomic force microscope (AFM) has been used to apply such forces, but large membrane perturbations occurring in vivo are also treated within the same framework. Inclusions of this nature may include cell junctions, filipodia, caveolae, and similar membrane invaginations. The breakdown of linear elastic response, as observed by AFM, is predicted to occur for forces as small as 10 pN. We estimate the position of this crossover and the subsequent nonlinear behavior and make encouraging quantitative comparison with experiments. Intrinsic membrane inclusions interact through their overlapping strain fields. For similar, point force-like inclusions at large separations, this yields an attractive potential that scales like the inverse of their separation. For membranes that are intrinsically stiff or under tension, the binding force between inclusions can depend on the properties of the membrane and may be large enough to induce aggregation of inclusions, as observed experimentally. For inclusions that fix the magnitude of the membrane deformation, rather than the applied force, we demonstrate the possibility of metastable states, corresponding to finite separations. Finally, we discuss briefly the case in which inclusions couple to the membrane in more complex ways, such as via a torque (twist). In such cases, the interaction scales like a higher power of the separation, depends on the orientation of the inclusions, and can have either sign.

INTRODUCTION

Biological membranes play many essential roles in nature and are found in all animal and plant cells (Alberts et al., 1994; Darnell et al., 1990). The cytoplasmic membrane is connected to a network made up of the microtubules, the microfilaments, and the intermediate filaments in a complex way that is still not fully understood. This network may often dominate the rheological, or mechanical, behavior of the cell (Thoumine and Ott, 1997; Janmey et al., 1991, 1994; Mackintosh et al., 1995). The plasma membrane itself has both an intrinsic rigidity and an osmotically driven surface tension (Sheetz and Dai, 1996). It is therefore surprising that, to our knowledge, there have been no theoretical studies of the deformation of such membranes coupled to elastic media other than one, somewhat different study that appeared after submission of the present work (Boulbitch, 1998). Quantitative measurements of the cellular response may best be performed by direct experimental probes (Evans et al., 1995), such as the atomic force microscope (AFM), in which the forces exerted on microscopic tip(s) in contact with a surface can be measured with accuracy. Indeed, several such experiments have been conducted on intact cells (A-Hassan et al., 1998; Haydon et al., 1996; Henderson 1994; Kasas et al., 1993; Radmacher et al., 1996). We will show that our theoretical predictions are in both qualitative and quantitative agreement with some of these measurements.

We also envisage a theoretical model for the interactions between intrinsic membrane inclusions that distort the membrane. Forces may be applied to the membrane by inclusions involved in either 1) cell adhesion, such as gap and spot junctions (desmosomes), 2) cytoskeletal changes, such as filipodia formation (Henderson et al., 1992; Sheetz et al., 1992), or 3) membrane invaginations, such as clathrin-coated pits and caveolae (Rothberg et al., 1992), which are, in turn, thought to be caused by aggregating membrane proteins (Schekman and Orci, 1996). Aggregation of these inclusions sometimes occurs, implying the existence of attractive forces. For example, the numerous actin filaments in filipodia localize (aggregate) so as to distort the plasma membrane. Furthermore, small aggregates of gap junctions and caveolae are often observed. There are many possible origins for the attractive forces acting between these inclusions. One may be the mechanical distortion of the cell surface and interior, as studied here, although specific molecular interactions may often be important.

In recent years, numerous studies of intrinsic membrane inclusions have been undertaken by scientists interested in their physics (Huang, 1986; Shen et al., 1993; Dan et al., 1993, 1994; Nallet et al., 1994; Palmer et al., 1994; Bruinsma et al., 1994; Netz and Pincus, 1995; Bar-Ziv et al., 1995; Aranda-Espinoza et al., 1996; Nicot et al., 1996; Turner and Sens, 1997, 1998; Sens et al., 1997; Goulian et al., 1993). Many of these have been motivated, at least in part, by similarities with biological membranes. However, any discussion of bulk elastic effects has been omitted in these articles. This omission provides further motivation for the present work.

We seek a model both for the elastic response of the membrane to localized deformation and for the interactions between inclusions such as those described above. These will be mediated by the elastic deformation of both the membrane and the elastic medium to which it is anchored. Such interactions may dramatically effect both aggregation and diffusion processes. Interacting diffusant particles will exhibit anomalous diffusion, perhaps similar to that exhibited by neural cell adhesion molecules, which are corraled (Simson et al., 1998). A picture of some highly idealized inclusions is given in Fig. 1.

In what follows we treat the medium as infinite, homogeneous, and purely elastic. Anchored to this medium is a fluid membrane bearing inclusions. We need not be specific
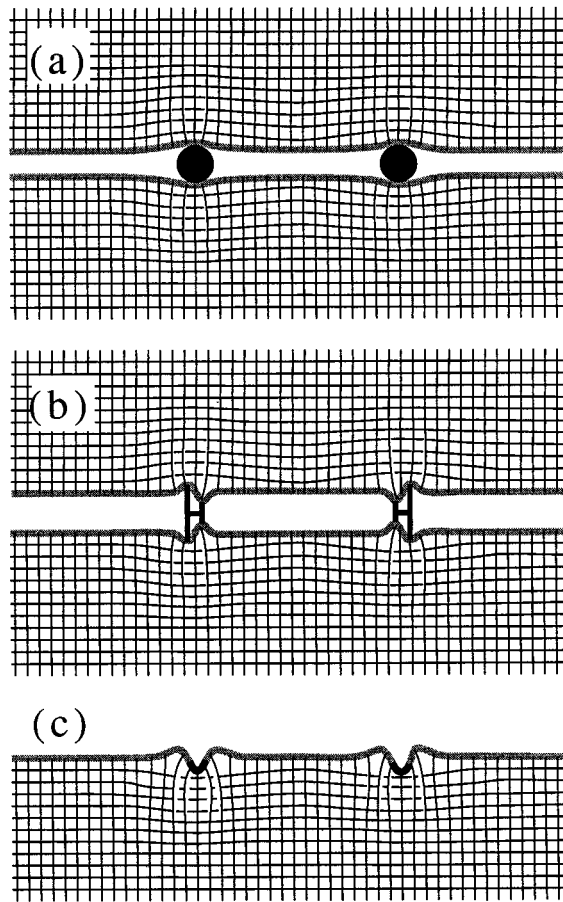

FIGURE 1 Schematic plot of three types of inclusions. These may represent either external probes, e.g., an AFM tip, or intrinsic inclusions, e.g., membrane invaginations, gap junctions, etc. In each case, the overlapping strain fields give rise to an interaction between any two inclusions. The thick shaded line represents the membrane(s) and the network of thin black lines the strained elastic medium. Three different types of inclusions are shown although *b* and *c* are discussed only in the appendix. (*a*) Those that exert a finite normal force. In the limit where the membranes are negligible, this system has the classical analogue of two ballbearings lying on a rubber slab. (*b*) Those that exert a finite local torque but no average normal force (a "dipole"). (*c*) Those that induce a finite local curvature but no average normal force or tilt (a "quadrupole"). In both *a* and *b* the inclusions are shown anchored to a second slab, which balances the normal forces and torques, respectively.

as to the nature of these inclusions; they are initially assumed merely to exert fixed normal forces on the membrane. We subsequently study the case where the inclusions fix the magnitude of the local membrane deformation. We neglect dynamic effects associated with cytoskeletal reorganization, leading to viscoelastic response. We believe that this approach is reasonable on short enough time scales (see Discussion and Conclusions). In any case, it is a natural starting point and may be achieved directly in well controlled artificial systems involving cross-linked polymer gels.

Our main results are as follows. 1) For a single, localized, force linear response breaks down when the applied force exceeds a critical value. This value scales linearly with the bulk elastic modulus and with the square of the largest of several microscopic cutoff lengths. 2) Well above this crossover the force is predicted to exhibit a quadratic dependence on the displacement. 3) Two inclusions that exert fixed normal forces on the membrane in the same direction (either up or down) attract one another. 4) The total binding energy of two inclusions brought together from infinity will depend on the properties of the membrane for sufficiently stiff membranes. 5) For large separations, the interaction potential is dominated by elastic stresses in the bulk medium and scales like $1/r$. 6) Our results are relatively insensitive to the choice of fixed-deformation or fixed-force boundary conditions only in the far-field limit and may be quite different for smaller separations. 7) Fixed-deformation boundary conditions, which may be appropriate for certain inclusions, can give rise to metastable states at finite separation. 8) For inclusions that induce curvature in the membrane, the leading order moment of the force distribution is the quadrupole and the interaction potential scales like $1/r^5$.

This paper is organized as follows. First, we present a theoretical model for weak distortions to a membrane anchored to an elastic medium. Next, we study the effects of inclusions that exert fixed localized normal forces on these membranes. Focusing on the case of a single inclusion, we compare our predictions to experiment. We consider also the case of fixed deformation boundary conditions. Finally, we discuss the significance of our results and some of the limitations of our highly idealized model. An appendix is also included in which we discuss how to extend the results to more complex inclusions by identifying an analogy between the total force exerted by the inclusion and electrostatic charge. In this analogy, the dipole, quadrupole, and higher-order moments correspond, as usual, to ascending moments of the force (charge) distribution.

WEAK DEFORMATIONS OF THE ANCHORED MEMBRANE

To describe the effect of localized inclusions we first construct the Hamiltonian for a general, weak deformation. We review the classical result for a semi-infinite elastic medium and then introduce a fluid membrane to obtain the Hamiltonian for the combined system.

Consider first a bare semi-infinite elastic medium confined to $z > 0$. By bare we mean a medium that does not yet support a membrane or any other structure. In what follows we will model the deformation of this medium by linear elastic theory (Landau and Lifshitz, 1981). This involves assuming that the medium is uniform, i.e., homogenous and isotropic, and that the applied deformation is sufficiently weak so that the response is linear. Thus, Hooke's law (restoring force is proportional to deformation) is assumed to hold when suitably generalized to a three dimensional (3-D) medium. In 3-D, a scalar extension, such as would describe a spring, is no longer adequate and one must use instead the strain tensor

$$\eta_{ij} = \frac{1}{2}\left(\frac{\partial \eta_i}{\partial x_j} + \frac{\partial \eta_j}{\partial x_i}\right) \tag{1}$$

where η_i is the ith component of the vector displacement of a point in the material and x_i is its ith Cartesian coordinate. The appropriate version of Hooke's law is a linear relation between the stress tensor σ_{ij} and the strain tensor

$$\sigma_{ij} = \frac{E}{1 + \sigma}\left(\eta_{ij} + \frac{\sigma}{1 - 2\sigma}\eta_{kk}\delta_{ij}\right), \tag{2}$$

where E is Young's modulus and σ Poisson's ratio for the elastic medium. The use of the same symbol (σ) for both Poisson's ratio and the stress tensor is unfortunate but conventional. Confusion should not arise as Poisson's ratio is a scalar whereas the stress is a second-rank tensor, bearing two additional indices.

At equilibrium, the internal stresses (forces) in every volume element must balance exactly:

$$\frac{\partial \sigma_{ij}}{\partial x_j} = 0 \tag{3}$$

Solving this equation for the deformation u of the surface of the semi-infinite medium in the z-direction due to a normal force f (per unit area) applied at this surface we find (Landau and Lifshitz, 1981)

$$u(\mathbf{r}) = \int d^2\mathbf{r}'(G(\mathbf{r} - \mathbf{r}')f(\mathbf{r}') \tag{4}$$

where $\mathbf{r}$ and $\mathbf{r}'$ are vectors in the x-y plane. The far-field deformation due to a normal force is well described by the following Green's function:

$$G(\mathbf{r}) = \frac{1}{2\pi\mathscr{E}}\frac{1}{|\mathbf{r}|} \tag{5}$$

The similarity between this expression and the Coulomb potential for point charges immediately invites an analogy with electrostatics. Here f plays the role of charge and u of the electrostatic potential. However, $\mathscr{E}$ is not a permittivity

but a rescaled elastic modulus given by

$$\mathscr{E} = \frac{E}{2(1 - \sigma^2)} \tag{6}$$

By analogy with electrostatics or otherwise it is straightforward to show that the total elastic potential energy of deformation is

$$U_{el} = \frac{1}{2}\int\int d^2\mathbf{r}d^2\mathbf{r}'f(\mathbf{r})f(\mathbf{r}')G(\mathbf{r} - \mathbf{r}') \tag{7}$$

It will often prove convenient to rewrite this in Fourier space defined by the transform

$$u(\mathbf{r}) = \int \frac{d^2\mathbf{q}}{(2\pi)^2}u_{\mathbf{q}}e^{i\mathbf{q}\mathbf{r}} \tag{8a}$$

and its inverse

$$u_{\mathbf{q}} = \int d^2\mathbf{r}u(\mathbf{r})e^{-i\mathbf{q}\mathbf{r}} \tag{8b}$$

In this space, Eq. 4 becomes

$$u_{\mathbf{q}} = G_{\mathbf{q}}f_{\mathbf{q}} \tag{9}$$

For such a semi-infinite elastic medium $G_{\mathbf{q}} = 1/(\mathscr{E}q)$ with $q \equiv |\mathbf{q}|$ throughout. Writing Eq. 7 as a function of u in reciprocal space we obtain the energy of the deformed elastic medium

$$U_{el} = \frac{1}{2}\int \frac{d^2\mathbf{q}}{(2\pi)^2}\mathscr{E}qu_{\mathbf{q}}u_{-\mathbf{q}} \tag{10}$$

Equipped with this result we now turn to the problem of a thin fluid membrane anchored to the surface of a semi-infinite elastic medium. An important simplifying feature of the problem is that such a fluid membrane transmits only normal stresses.

We consider first an isolated membrane with surface tension γ and intrinsic bending rigidity κ. The deformation energy of the membrane is

$$U_{memb} = \int d^2\mathbf{r}\left[\frac{\kappa}{2}(\nabla_{\parallel}^2 u)^2 + \frac{\gamma}{2}(\nabla_{\parallel}u)^2\right]$$

$$= \frac{1}{2}\int \frac{d^2\mathbf{q}}{(2\pi)^2}[\kappa q^4 + \gamma q^2]u_{\mathbf{q}}u_{-\mathbf{q}}, \tag{11}$$

where $\nabla_{\parallel}$ is the gradient operator in the x-y plane.

The total energy of deformation of the membrane and the elastic substrate is merely $U_{def} = U_{el} + U_{memb}$:

$$U_{def} = \frac{1}{2}\int \frac{d^2\mathbf{q}}{(2\pi)^2}\frac{u_{\mathbf{q}}u_{-\mathbf{q}}}{G_{\mathbf{q}}}, \tag{12}$$

with the Greens function in the presence of the membrane now given in **q**-space by

$$G_{\mathbf{q}} = \frac{1}{\mathscr{E}q + \gamma q^2 + \kappa q^4} \tag{13}$$

Of course, the membrane modifies the real space response function $G(\mathbf{r})$ too. This is now given by the inverse Fourier transform of Eq. 13. The Greens function Eq. 5 is recovered in the limit $\gamma, \kappa \to 0$. Relationships of the form of Eqs. 10, 11, and 12 are often encountered in statistical mechanics although here we are interested in deformations that are much larger than thermal fluctuations. Hence our identification of a potential energy rather than a free energy.

Effect of membrane inclusions

To understand the behavior of localized inclusions the field $f(\mathbf{r})$ can be thought of either as the force per area due to some distribution of inclusions or, alternatively, as a Lagrange field chosen to impose some unspecified boundary condition on the distortion field $u(\mathbf{r})$. These interpretations correspond to the two boundary conditions, fixed force and fixed deformation, considered below, although in both cases we introduce the membrane-inclusion coupling into the energy as follows

$$F = \frac{1}{2}\iint d^2\mathbf{r}d^2\mathbf{r}' u(\mathbf{r})u(\mathbf{r}')\mathscr{G}(\mathbf{r} - \mathbf{r}') - \int d^2\mathbf{r}u(\mathbf{r})f(\mathbf{r}), \tag{14}$$

where $\mathscr{G}(\mathbf{r})$ is the Fourier transform of $1/G_{\mathbf{q}}$. Minimizing this in **q**-space by completing the square we have

$$F = -\frac{1}{2}\int\frac{d^2\mathbf{q}}{(2\pi)^2}G_{\mathbf{q}}f_{\mathbf{q}}f_{-\mathbf{q}}, \tag{15}$$

which gives the total energy as a function of the field f. The (positive) total energy of deformation can be shown to be $U_{\mathrm{def}} = -F$ with the minus sign indicating that f is driving the deformation. The relationship $U_{\mathrm{def}} = -F$ is characteristic of elastic response; it holds for a Hookean spring extended by a constant force.

For the purposes of calculating the two-body interaction potential we will write $f(\mathbf{r}') = \psi(\mathbf{r}') + \psi(\mathbf{r} - \mathbf{r}')$ where $\mathbf{r}$ is the vector separating the two inclusions and $\psi(\mathbf{r}')$ is the force density distribution for a single inclusion centered at the origin. In the far-field limit we will see that the interaction potential between two inclusions, as well as the deformation energy of a single one, will depend only on the total force $\psi_{\mathrm{o}} = \int d^2\mathbf{r}' \psi(\mathbf{r}')$. In the fixed-deformation boundary conditions, the field ψ, and hence ψ_{o}, will further depend implicitly on $\mathbf{r}$. This is necessary to fix the magnitude of the deformation for all separations. In the fixed-force boundary conditions, ψ_{o} is taken to be a fixed constant, with no implicit r-dependence. This is the essence of the difference between these two natural choices of bound-

ary condition. Both choices turn out to give similar interaction potentials when the inclusions are identical, with merely a different numerical prefactor.

FIXED-FORCE BOUNDARY CONDITIONS

In this section we consider two inclusions, separated by r, exerting fixed localized normal forces on the membrane. From Eq. 15 we have

$$F = -\int\frac{d^2\mathbf{q}}{(2\pi)^2}G_{\mathbf{q}}(1 + e^{i\mathbf{q}\mathbf{r}})\psi_{\mathbf{q}}\psi_{-\mathbf{q}}, \tag{16}$$

which is made up of the sum of a constant term, corresponding to a self energy per inclusion,

$$F^{(s)} = -\frac{1}{2}\int\frac{d^2\mathbf{q}}{(2\pi)^2}G_{\mathbf{q}}\psi_{\mathbf{q}}\psi_{-\mathbf{q}}, \tag{17}$$

and an **r**-dependent term giving the two-body interaction potential per inclusion,

$$\phi(\mathbf{r}) = -\frac{1}{2}\int\frac{d^2\mathbf{q}}{(2\pi)^2}G_{\mathbf{q}}e^{i\mathbf{q}\mathbf{r}}\psi_{\mathbf{q}}\psi_{-\mathbf{q}} \tag{18}$$

$$= -\frac{1}{2}\int d^2\mathbf{r}'\int d^2\mathbf{r}''G(\mathbf{r} - \mathbf{r}' - \mathbf{r}'')\psi(\mathbf{r}')\psi(\mathbf{r}'')$$

Thus, the self energy is related to the interaction potential by the following equivalence:

$$F^{(s)} = \phi(\mathbf{r} \to 0) \tag{19}$$

For separations $r \gg b$, where b is a microscopic length of the order of the lateral size of an inclusion, the inclusions can be thought of as point particles. (This gives the dominant far-field term for finite ψ_{o} (but see the Appendix for a discussion of higher-order effects). Here we simply notice $\psi_{\pm\mathbf{q}} \approx \psi_{\mathrm{o}}$ for $q \ll b^{-1}$ and vanishes in the large q limit. The length b is equal to the lateral size of the inclusion up to a shape-dependent prefactor of order unity. In what follows we will furthermore assume that b is larger than the characteristic cytoskeleton mesh size ξ.) Hence,

$$\phi(\mathbf{r}) = -\frac{1}{2}\psi_{\mathrm{o}}^2 G(\mathbf{r}) \quad \text{for } r \gg b \tag{20}$$

Substituting $x = qr$, the real space Greens function $G(\mathbf{r})$ is given by

$$G(\mathbf{r}) = \frac{1}{2\pi\mathscr{E}r}\int_0^{\infty}\frac{J_{\mathrm{o}}(x)dx}{1 + \frac{1}{2}(x/x_{\gamma}) + \frac{1}{2}(x/x_{\kappa})^3}, \tag{21}$$

where $J_{\mathrm{o}}(x)$ is the Bessel function of the first kind of order 0, $x_{\gamma} = r/l_{\gamma}$ and $x_{\kappa} = r/l_{\kappa}$, with the two characteristic lengths given by

$$l_{\gamma} = \gamma/\mathscr{E} \quad \text{and} \quad l_{\kappa} = (\kappa/\mathscr{E})^{1/3} \tag{22}$$

A plot of the interaction potential Eq. 20 is shown in Fig. 2. In the limit of large particle separations $r \gg l_\gamma, l_\kappa$, the interaction potential per particle becomes simply

$$\phi(\mathbf{r}) = -\frac{\psi_o^2}{4\pi \mathscr{E} r} \qquad (23)$$

For separations that are less than l_γ or l_κ, the potential crosses over to

$$\phi(\mathbf{r}) = \begin{cases} -\dfrac{\psi_o^2}{4\pi \mathscr{E} l_\gamma} \log(l_\gamma/r) & \text{if } l_\gamma \gg l_\kappa \text{ and } r \ll l_\gamma \\[2ex] -\dfrac{\psi_o^2}{6\sqrt{3}\mathscr{E} l_\kappa} & \text{if } l_\kappa \gg l_\gamma \text{ and } r \ll l_\kappa, \end{cases} \qquad (24)$$

where we have assumed that the intrinsic size of the inclusion is smaller than these new length scales; if not, then it is, rather, b that appears as the natural short length cutoff, e.g., for Eq. 23. The logarithmic term appearing in Eq. 24 is never large. (The apparent logarithmic singularity as $r \to 0$ will be the cutoff either by the appearance of higher-order terms in the Hamiltonian, which start to become important on length scales $r \lesssim \psi_o/\gamma$, or by the effect of the bending rigidity at $r \simeq l_\kappa$, or by additional short-range forces, ultimately including steric contact.) Note the similarity of Eq. 23 with the usual result for the electrostatic potential (per inclusion) between two charges of magnitude ψ_o. This result indicates that for large enough separations the deformation of the bulk elastic medium dominates the interactions.

The above arguments hold for inclusions that are sufficiently far apart for linear elasticity theory to remain adequate. Specifically, we do not accurately take account of any strains in the elastic medium (or gradient at the surface) greater than or of the order of unity. It can be shown that
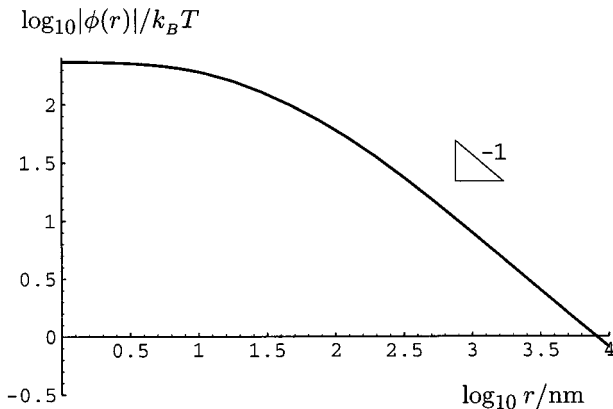
$\log_{10}|\phi(r)|/k_B T$

FIGURE 2 The absolute value of ϕ, the interaction potential between two inclusions, as a function of their separation r as calculated numerically from Eqs. 20 and 21. The parameters used are $l_\gamma = 200$ nm, $l_\kappa = 30$ nm, $\psi_o = 20$ pN, and $\mathscr{E} = 1$ kPa with b assumed negligible. The far-field asymptotic $1/r$ behavior is clearly visible, as is the crossover around l_γ, which is here the largest cutoff length. Using Eq. 28, the normal membrane deflection is estimated to be ~16 nm.

these strains are always smaller than unity far enough away from an inclusion $r \gtrsim l_{\mathscr{E}}$, where

$$l_{\mathscr{E}} = \sqrt{\psi_o/\mathscr{E}} \qquad (25)$$

Beyond this length the elastic response of a single inclusion is well known and corresponds to the Hertz model (Hertz, 1881). However, the effect of the breakdown of linearity for $r \lesssim l_{\mathscr{E}}$ is to fundamentally modify the elastic response, as we will show below. In the present work we consider only the contribution of the far field to both the interactions and self energy, neglecting any "core" corrections due to non-linear or other short-ranged interactions. Crudely speaking, we can think of $l_{\mathscr{E}}$ as being another short-length cutoff for our theory in what follows. Hence we can obtain an estimate of the self energy $F^{(s)}$, also equal to the change in energy when a pair of inclusions is brought together from infinity, by setting $r = l_{\text{big}}$ in Eq. 23 where l_{big} is the largest of the lengths b, $l_{\mathscr{E}}$, l_γ, or l_κ. From Eqs. 22–25 we find

$$F^{(s)} \simeq \begin{cases} -\psi_o^2 \mathscr{E}^{-1} b^{-1} & \text{if } b \gg l_\gamma, l_\kappa, l_{\mathscr{E}} \\ -\psi_o^2 \gamma^{-1} & \text{if } l_\gamma \gg l_\kappa, l_{\mathscr{E}}, b \\ -\psi_o^2 \kappa^{-1/3} \mathscr{E}^{-2/3} & \text{if } l_\kappa \gg l_\gamma, l_{\mathscr{E}}, b \\ -\psi_o^{3/2} \mathscr{E}^{-1/2} & \text{if } l_{\mathscr{E}} \gg l_\gamma, l_\kappa, b, \end{cases} \qquad (26)$$

where the numerical prefactors depend on the precise way in which we cut off at short length scales. In general, these are difficult to estimate as they depend on the full nonlinear Hamiltonian and/or other short-range interactions. (The prefactor may be given precisely only in the third limit ($l_\kappa \gg l_\gamma, l_{\mathscr{E}}, b$). In this case, it is $1/(6\sqrt{3})$. In both other limits, it depends at least logarithmically on the precise cutoff employed.) However, we will make a crude estimate of the magnitude of $F^{(s)}$ in the next section. At thermodynamic equilibrium, inclusions that are free to move laterally will form aggregates if this energy is much larger than the entropic contribution $k_B T |\log c|$, where c is the area fraction of inclusions on the membrane. Whether such aggregation occurs *in vivo* will also depend on other factors, e.g., whether the time scale for aggregation is less than that of the reorganization of the cytoskeleton, as discussed in the Discussion and Conclusions.

Single inclusion

Before discussing the interactions between inclusions we will examine the effect of a single inclusion. The single-inclusion distortion field u is entirely determined by Eq. 9 and Eq. 13 with $f = \psi$. Thus, we are in a position to make quantitative predictions for the deflection of the membrane as a function of applied force. AFM measurements of the deflection of the surface of human platelets already exist (Radmacher et al., 1996), and later in this section we will compare our predictions with these data. As discussed below, the agreement is most encouraging.

The maximal normal deformation of the membrane near an isolated inclusion, written $\bar{u}$, is related to the force

applied on it according to the mechanical equilibrium condition

$$\frac{\partial F^{(s)}}{\partial \bar{u}} = \psi_o \qquad (27)$$

The self energy $F^{(s)}$ is given by Eq. 23 with an appropriate small-length-scale cutoff, as discussed above. Thus, Eq. 27 is a first-order differential equation relating the force ψ_o to the displacement $\bar{u}$. Using the approximate cutoff $r = l_{\text{big}}$ in Eq. 23, we obtain

$$\psi_o = \begin{cases} 2\pi\mathscr{E}b\bar{u} & \text{if } b \gg l_\gamma, l_\kappa, l_\mathscr{E} \\ 2\pi\gamma\bar{u} & \text{if } l_\gamma \gg l_\kappa, l_\mathscr{E}, b \\ 2\pi\kappa^{1/3}\mathscr{E}^{2/3}\bar{u} & \text{if } l_\kappa \gg l_\gamma, l_\mathscr{E}, b \\ (4\pi/3)^2\mathscr{E}\bar{u}^2 & \text{if } l_\mathscr{E} \gg l_\gamma, l_\kappa, b, \end{cases} \qquad (28)$$

which represents a relationship between the force and the membrane deflection. It should be emphasized that the numerical prefactors are estimates arising from our treatment and should be regarded as approximate. They are included merely to facilitate the comparison with experimental data presented later in this section.

The last of the results contained in Eq. 28 may seem the most surprising. It says that the system no longer behaves in a linear Hookean way if $l_\mathscr{E}$ is the largest cutoff length. As $l_\mathscr{E}$ increases with the applied force according to Eq. 25, whereas the other lengths remain constant, this behavior will dominate at high forces. Thus, we predict a crossover from linear variation of ψ_o with $\bar{u}$ to one that is quadratic in $\bar{u}$ when $l_\mathscr{E} \gtrsim l_2$ where l_2 is the largest of b, l_γ, or l_κ. This can be shown to occur for forces larger than ψ_{o_c} or, equivalently, displacements larger than $\bar{u}_c$ given by

$$\psi_{o_c} \simeq \mathscr{E}l_2^2 \qquad \bar{u}_c \simeq l_2 \qquad (29)$$

The origin of this crossover is the breakdown of linear elasticity theory in the vicinity of the inclusion for such large forces. Our approximate treatment of this breakdown involves neglecting any distortion of this region beyond this limit. This is probably reasonable provided higher-order terms in the Hamiltonian give rise to a significant stiffening of the material beyond this crossover and there is no mechanical failure of the material (cytoskeleton). A likely lower estimate of the force might correspond to parameter values of $\mathscr{E} \approx 1$ kPa and $l_2 \approx 100$ nm giving $\psi_{o_c} \gtrsim 10$ pN.

The energy $F^{(s)}$ as a function of deformation follows trivially from Eq. 28:

$$F^{(s)} \simeq \begin{cases} -\pi\mathscr{E}b\bar{u}^2 & \text{if } b \gg l_\gamma, l_\kappa, l_\mathscr{E} \\ -\pi\gamma\bar{u}^2 & \text{if } l_\gamma \gg b, l_\kappa, l_\mathscr{E} \\ -\pi\kappa^{1/3}\mathscr{E}^{2/3}\bar{u}^2 & \text{if } l_\kappa \gg b, l_\gamma, l_\mathscr{E} \\ -\dfrac{(4\pi)^2}{3}\mathscr{E}\bar{u}^3 & \text{if } l_\mathscr{E} \gg b, l_\gamma, l_\kappa \end{cases} \qquad (30)$$

The physical interpretation of these results is as follows: 1) In systems where $l_\gamma \gg b$, l_κ, $l_\mathscr{E}$ most of the deformation energy comes from the work done in stretching the membrane against surface tension. 2) In systems where $l_\kappa \gg b$,

l_γ, $l_\mathscr{E}$ most of it comes from the work done in bending the membrane. 3) In systems where $l_\mathscr{E}$ or b are largest the effect of the membrane is negligible and most of the deformation energy is the work done in elastically deforming the medium.

A conservative estimate of $F^{(s)}$ for intrinsic membrane inclusions might be obtained from Eq. 30 using $\mathscr{E} = 1$ kPa, $b = 30$ nm, and $\bar{u} = 10$ nm. These values give $F^{(s)} = 10^{-22}$ J $= 2.5$ $k_B T$, which are thermodynamically significant.

Comparison with experiment

As mentioned above, there exist several AFM measurements of the surface of living cells. One of these studies (Radmacher et al., 1996) represents perhaps the best data available for our purposes. (See Fig. 6, p 560 in Radmacher et al., 1996. When interpreting these data we use the average force measured over several approaches and retractions at low frequencies 0.2–20 Hz. These frequencies probably represent time scales that are sufficiently short so that effects associated with cytoskeleton reorganization may be neglected, whereas at the same time being rather long compared with the fluid relaxation times $\tau \simeq \eta l_{\text{big}}^2/\psi_o \approx 100$ μs.) (See Fig. 3). In this experimental work an AFM tip is pressed into the surface of a human platelet. As usual, the force is measured optically via the displacement of an extremely soft cantilever supporting the tip. These authors report that their cantilever has a spring constant $k = 31$ pN/nm and a physical tip size of the order of $b = 50$ nm. Their data show an approximately linear regime, with the cantilever deflection d proportional to the vertical sample displacement, followed by a regime where the deflection shows a sudden and marked deviation from linear response toward behavior approximately quadratic in the displace-
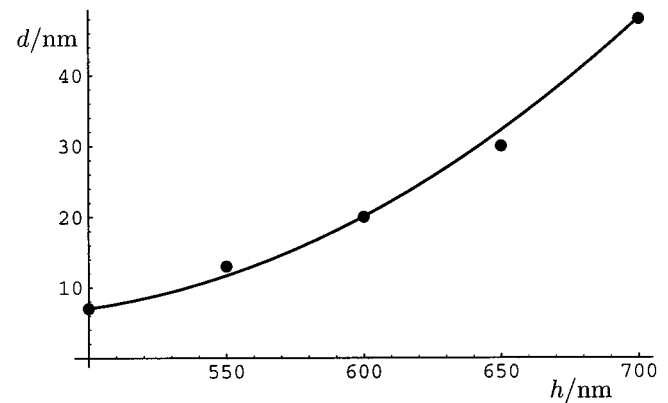
FIGURE 3 The AFM cantilever deflection d plotted against the stage height h reported in Radmacher et al., 1996. The stage height h is identified with the membrane deflection $\bar{u}$, and the displacement d is proportional to the force with a Hooke's constant $k = 31$ pN/nm. The data points are extracted by eye from the continuous trace data and fitted to a general quadratic form (—). The curvature m of this fit allows a second estimate of the elastic modulus in good agreement with that obtained from linear response, as discussed in the text. The quadratic form is a key prediction of our model and fits the data well.

ment. This is in qualitative agreement with the behavior predicted by us.

We first estimate the elastic modulus of the material from the slope of the linear portion of the force-versus-displacement curve. The force exerted by the arm must balance that of the membrane Eq. 28 according to $kd = 2\pi\mathcal{E}b\bar{u}$, where we assume $b > l_\gamma, l_\kappa$. (For $\kappa \lesssim 10k_BT$ we find $l_\kappa \lesssim 30$ nm. The surface tension has been reported to be in the range 10^{-2} to 10^{-1} pN/nm (Sheetz and Dai, 1996) giving $l_\gamma \approx$ 10–100 nm.) Solving for $\mathcal{E}$ with $\bar{u} = 500$ nm, $b = 50$ nm, $d = 7$ nm, and $k = 31$ pN/nm we find $\mathcal{E} = 1.4$ kPa, in good agreement with the experimentally reported values of 1.5–4 kPa. This agreement is not surprising as the physics of the linear regime has long been well understood. However, it does verify that the approximate numerical prefactor in Eq. 28 is a rather good estimate. The force-versus-displacement curve crosses over from linear to approximately quadratic at $\bar{u} \approx 500$ nm. Our estimate from Eq. 29 is that this should occur when $\bar{u} \simeq b$, which indicates that the response should already be significantly nonlinear at these strains. Although our estimate is a little low, it is roughly of the right order of magnitude and is encouraging given the crude nature of our estimate. Perhaps more encouraging still is the existence of the crossover and its approximately quadratic form.

Finally, we can make a second estimate of $\mathcal{E}$ by extracting the *curvature* of the force-versus-displacement curve at high forces (see Fig. 3). Above the crossover, the data are well fitted by the expression $d - 6$ nm $= m(\bar{u} - 460$ nm$)^2$, yielding a curvature constant $m = 7.5 \times 10^{-4}$ nm^{-1}. Thus, for large displacements the force balance becomes

$$kd = km\bar{u}^2 = (4\pi/3)^2\mathcal{E}\bar{u}^2 \Rightarrow \mathcal{E} = 1.3 \text{ kPa}, \quad (31)$$

which is in excellent quantitative agreement with the estimate obtained from linear response. This, together with the nearly quadratic form above the crossover, represents the best evidence in support of our model.

FIXED-DEFORMATION BOUNDARY CONDITIONS

In the preceding section, we considered only one type of coupling between the inclusions and the membrane, i.e., that of a normal force of fixed magnitude. This is merely one of many possible choices. In some physical systems it may be more appropriate to fix the normal deformation near each inclusion as a boundary condition, i.e., require it to remain fixed even as they are brought together. To impose this boundary condition we should instead allow the force exerted by the inclusions to vary with the inclusion separation r in such a way as to correctly fix the deformation for all values of r. In this section, the case where the two inclusions are different, i.e., they exert different forces $\psi_o^{(1)}$ and $\psi_o^{(2)}$ when separated to infinity, will prove to be nontrivial. (For the case of fixed-force boundary conditions, it is merely the product of the forces $\psi_o^{(1)} \psi_o^{(2)}$, which enters as a prefactor to the interaction potential Eq. 20.)

After some algebra we find the interaction potential per particle

$$\phi'(r) = -\frac{1}{2}\psi_o^{(1)}\psi_o^{(2)}G(\mathbf{r})\left[\frac{1 - \frac{1}{2}\left(\frac{\psi_o^{(1)}}{\psi_o^{(2)}} + \frac{\psi_o^{(2)}}{\psi_o^{(1)}}\right)\frac{G(r)}{G(0)}}{1 - \left(\frac{G(r)}{G(0)}\right)^2}\right], \quad (32)$$

where the prime reminds us that we have employed fixed-deformation boundary conditions. Comparison of Eq. 32 with Eq. 20 confirms that the product of the two forces changes with r by the factor in Eq. 32 in square brackets, thereby keeping the magnitude of the deformation near both the inclusions constant.

In the far-field limit, the ratio $G(r)/G(0) \rightarrow l_{big}/r \rightarrow 0$ and Eq. 32 coincides with Eq. 23 up to corrections $O(l_{big}/r)$. This tells us that the interactions in the far-field limit are insensitive to the choice of boundary condition.

However, for $\psi_o^{(1)} \neq \psi_o^{(2)}$ the interaction potential $\phi'(r)$ exhibits a minimum for finite particle separation r_{min}. This separation is significantly larger than l_{big} only when $\psi_o^{(1)} \gg \psi_o^{(2)}$ (where $\psi_o^{(1)} > \psi_o^{(2)}$ without loss of generality) in which limit it approaches

$$r_{min} = l_{big}\psi_o^{(1)}/\psi_o^{(2)} \quad (33)$$

The interaction potential is locally quadratic about this minimum with restoring force per unit lateral displacement given by

$$\left.\frac{\partial^2\phi'}{\partial r^2}\right|_{r=r_{min}} = \frac{\psi_o^{(2)2}G(0)}{2l_{big}^2\left[\left(\frac{\psi_o^{(1)}}{\psi_o^{(2)}}\right)^2 - 1\right]} \quad (34)$$

and binding energy

$$\phi'(r_{min}) = -\tfrac{1}{4}\psi_o^{(2)2}G(0) \quad (35)$$

The self energy in this case is of no physical relevance. The result of Eq. 35 differs from the results of the preceding section only by a numerical prefactor of $\frac{1}{2}$.

In summary, we have found that there is only a small difference between the two choices of boundary condition for similar inclusions but that stable minima may appear in the two-body interaction potential for different inclusions under fixed-deformation boundary conditions.

DISCUSSION AND CONCLUSIONS

Our model is formulated in the limit of a uniform, infinite elastic medium. However, biological systems are notoriously complex. For finite and/or heterogeneous media, our results are accurate only over length scales smaller than the size of the domain in which $\mathcal{E}$ is roughly constant. However, it is plausible that the domain size of the cytoskeleton may reach the scale of the cell. If the membrane were to reside on a uniform elastic slab of finite thickness D, our results would remain valid for separations $r \ll D$. In the other

extreme, our theory will be appropriate for inclusion-induced deformation on a lateral scale larger than some characteristic mesh size for the cytoskeleton, which may be $\lesssim 0.1$ μm. On length scales smaller than this, our continuum approximation for the medium will start to break down. Thus, there exists a regime of applicability of perhaps two orders of magnitude or more.

We might hope to include some dynamic effects by treating the medium as viscoelastic. Although some work exists for surface waves on a viscoelastic medium (Pleiner et al., 1988; Harden et al., 1991; Safran and Klein, 1993), our results are probably sensitive to the nature of the bulk network, and a full dynamic theory is, in any case, outside the scope of the present work. However, we can say that we do expect our results to be appropriate for systems in which stress relaxes sufficiently slowly. Encouragingly, recent experimental work on the scale of a cell (Thoumine and Ott, 1997) determined a characteristic time of the order of 40 s. For times much less than this, the cell appears to behave elastically. This time may be two orders of magnitudes larger than, e.g., the characteristic time for a typical membrane protein to diffuse over the scale of a cell.

We have presented evidence that linear elastic theory is inadequate to describe the response of a cell to forces in excess of some critical value. For the data set discussed in the text, this force was of the order of 200 pN but may be as small as 10 pN for other systems. Above this crossover we 1) predict that the force varies quadratically with the displacement and 2) are able to make a second independent prediction of $\mathscr{E}$ from the curvature of the quadratic form in this regime. For the data set examined, a quadratic response does seem to be closely followed, and both estimates of the elastic modulus agree remarkably well. Together these observations represent the best evidence that our model correctly describes the response of the system up to and beyond the breakdown of linear elasticity.

Finally, we may conclude as follows. By considering the elastic length $l_{\mathscr{E}}$ we have been able to model the response of a membrane anchored to an elastic medium to applied forces up to and beyond the breakdown of linear elasticity. Such inclusions interact with one another with a far-field potential scaling like $1/r$ provided that they exert some mean force. For sufficiently stiff or taut membranes, their response to applied forces depends on the properties of the membrane. For inclusions that fix the magnitude of the membrane deformation, rather than the applied force, we have demonstrated the possibility of metastable states corresponding to inclusions at finite separation.

APPENDIX

The inclusions considered in the main body of the text are all assumed to exert localized normal forces on the membrane. As mentioned in the Introduction, we may employ a multipole expansion, analogous to that of classical electrostatic theory, to model more complex force distributions. A thorough description of this technique exists in the context of inclusions in a multi-layered lamellar phase (Turner and Sens, 1998). In the current work, charge is analogous to $\psi_o = \int \psi(\mathbf{r}')d^2\mathbf{r}'$, dipole moment to $\mathbf{p} = \int \mathbf{r}' \psi(\mathbf{r}')d^2\mathbf{r}'$, quadrupole moment to $\mathscr{D}_{ij} = \int r_i'r_j'\psi(\mathbf{r}')d^2\mathbf{r}'$, etc.

Each of the moments of ψ has a physical interpretation as follows. The charge is merely the total force exerted on the membrane ψ_o. Thus, for inclusions with a finite charge, the distribution of this charge enters as a higher-order correction only for inclusions with sizes much smaller than their separation. Inclusions with a finite dipole moment induce a tilt in the membrane. This may be visualized by viewing a dipole as a point-upward and a point-downward force separated by some small distance. A pure dipole has no finite normal force (displacement). Finally, the quadrupole moment acts to induce curvatures in the membrane but has no finite normal force or torque (tilt). Inclusions in this class have an interaction potential that varies like $1/r^5$, as argued below, but need not have a binding energy that is qualitatively different from those that exert finite normal forces (or torques). Such curvature-inducing inclusions have been studied in the context of fluid membrane systems (Goulian et al., 1993). Although this earlier work also predicts power-law interactions, it differs fundamentally from the present work in that 1) there is no bulk elastic medium through which interactions may be mediated and 2) it also includes a treatment of fluctuations, appropriate for very soft systems, whereas we do not.

The interaction potential between higher-order poles is easily obtained by analogy with electrostatics directly from Eq. 18. As the two inclusions need not be identical, the first and second inclusions and their moments are labeled 1 and 2, respectively. Thus, the interaction potential between two point charge inclusions separated by $\mathbf{r}$ is $\phi(\mathbf{r}) = -\frac{1}{2}\psi_o^{(1)}\psi_o^{(2)} G(\mathbf{r}) \sim 1/r$; between two point dipole inclusions, it is $\psi(\mathbf{r}) = \frac{1}{2}p_i^{(1)}p_j^{(2)}\nabla_i\nabla_j G(\mathbf{r}) \sim 1/r^3$; and between two point quadrupoles, it is $\psi(\mathbf{r}) = -\frac{1}{8}\mathscr{D}_{kl}^{(2)}\nabla_i\nabla_j\nabla_k\nabla_l G(\mathbf{r}) \sim 1/r^5$. Extensions to higher-order and mixed moments, e.g., dipole-quadrupole interactions, are straightforward. Thus, we are able to treat quite general inclusions by calculating the moments of the field ψ. As we can always invert u to find ψ we might proceed as follows. From experimental evidence for the distortion field around an isolated inclusion, estimate u. From this, extract ψ and calculate its moments to obtain the far-field interaction potential and higher-order corrections to any order.

REFERENCES

A-Hassan, E., W. F. Heinz, M. D. Antonik, N. P. D'Costa, S. Nageswaran, C. A. Schoenenberger, and J. H. Hoh. 1998. Relative microelastic mapping of living cells by atomic force microscopy. *Biophys. J.* 74:1564.

Alberts, B., D. Bray, J. Lewis, M. Raff, K. Roberts, and J. D. Watson. 1994. Molecular Biology of the Cell. Garland, New York.

Aranda-Espinoza, H., A. Berman, N. Dan, P. Pincus, and S. Safran. 1996. Interactions between inclusions embedded in membranes. *Biophys. J.* 71:648–656.

Bar-Ziv, R., R. Menes, E. Moses, and S. A. Safran. 1995. Local unbinding of pinched membranes. *Phys. Rev. Lett.* 75:3356–3359.

Boulbitch, A. A. 1998. Deflection of a cell membrane under application of a local force. *Biophys. J.* 57:2123.

Bruinsma, R., M. Goulian, and P. Pincus. 1994. Self-assembly of membrane junctions. *Biophys. J.* 67:746–750.

Dan, N., A. Berman, P. Pincus, and S. A. Safran. 1994. Membrane-induced interactions between inclusions. *J. Phys.* 4:1713–1725.

Dan, N., P. Pincus, and S. A. Safran. 1993. Membrane-induced interactions between inclusions. *Langmuir.* 9:2768–2771.

Darnell, J., H. Lodish, and D. Baltimore. 1990. Molecular Cell Biology. Scientific American, New York.

Evans, E., K. Ritchie, and R. Merkel. 1995. Sensitive force technique to probe molecular adhesion and structural linkages at biological interfaces. *Biophys. J.* 68:2580–2587.

Goulian, M., R. Bruinsma, and P. Pincus. 1993. Long-range forces in heterogeneous fluid membranes. *Europhys. Lett.* 22:145–150.

Harden, J. L., H. Pleiner, and P. Pincus. 1991. Hydrodynamic surface modes on concentrated polymer solutions and gels. *J. Chem. Phys.* 94:5208–5221.

Haydon, P. G., R. Lartius, V. Parpura, and S. P. Marchese-Ragona. 1996. Membrane deformation of living glial cells using atomic force microscopy. *J. Microsc.* 182:114.

Henderson, E. 1994. Imaging of living cells by atomic force microscopy. *Prog. Surf. Sci.* 46:39.

Henderson, E., P. G. Haydon, and D. S. Sakaguchi. 1992. Actin filament dynamics in living glial cells imaged by atomic force microscopy. *Science.* 257:1944.

Hertz, H. 1881. Über den kontakt elastïscher körper. *J. Reine Angew. Mathematik.* 92:156.

Huang, H. 1986. Deformations free energy of bilayer membrane and its effect on gramicidin channel lifetime. *Biophys. J.* 50:1061–1070.

Janmey, P. A., U. Euteneuer, P. Traub, and M. Schliwa. 1991. Viscoelastic properties of vimentin compared with other filementatous biopolymer networks. *J. Cell Biol.* 113:155–160.

Janmey, P. A., S. Hvidt, J. Käs, D. Lerche, A. Maggs, E. Sackmann, M. Schliwa, and T. P. Stossel. 1994. The mechanical properties of actin gels: elastic modulus and filament motions. *J. Biol. Chem.* 269: 32503–32513.

Kasas, S., V. Gotzos, and M. R. Celio. 1993. Observation of living cells by atomic force microscopy. *Biophys. J.* 64:539.

Landau, L. D., and E. M. Lifshitz. 1981. Theory of Elasticity. Pergamon Press, Oxford.

MacKintosh, F. C., J. Käs, and P. A. Janmey. 1995. Elasticity of semiflexible biopolymer networks. *Phys. Rev. Lett.* 75:4425–4428.

Nallet, F., D. Roux, C. Quilliet, P. Fabre, and Milner, S. 1994. Elasticity and hydrodynamic properties of doped solvent dilute lamellar phases. *J. Phys.* 4:1477–1499.

Netz, R., and P. Pincus. 1995. Inhomogeneous fluid membranes: segregation, ordering and effective rigidity. *Phys. Rev. E.* 52:4114–4128.

Nicot, C., M. Waks, R. Ober, T. Gulik-Krzywicki, and W. Urbach. 1996. Squeezing of oil-swollen surfactant bilayers by a membrane protein. *Phys. Rev. Lett.* 77:3485–3488.

Palmer, K., M. Goulian, and P. Pincus. 1994. Fluctuation-induced forces in stacked fluid membranes. *J. Phys.* 4:805–817.

Pleiner, H., J. L. Harden, and P. Pincus. 1988. Surface modes on a viscoelastic medium. *Europhys. Lett.* 7:383–387.

Radmacher, M., M. Fritz, C. M. Kacher, J. P. Cleveland, and P. K. Hansma. 1996. Measuring the viscoelastic properties of human platelets with the atomic force microscope. *Biophys. J.* 70:556.

Rothberg, K. G., J. E. Heuser, W. C. Donzell, Y. Ying, J. R. Glenney, and R. G. W. Anderson. 1992. Caveolin, a protein component of caveolae membrane coats. *Cell.* 68:673–682.

Safran, S. A. 1994. Statistical Thermodynamics of Surfaces, Interfaces, and Membranes, Frontiers in Physics. Addison Wesley, New York.

Safran, S. A., and J. Klein. 1993. Surface instability of viscoelastic thin films. *J. Phys.* 3:749–757.

Schekman, R., and L. Orci. 1996. Coat proteins and vesicle budding. *Science.* 271:1526–1533.

Sens, P., M. S. Turner, and P. Pincus. 1997. Particulate inclusions in a lamellar phase. *Phys. Rev. E.* 55:4394–4405.

Sheetz, M. P., and J. W. Dai. 1996. Modulation of membrane dynamics and cell motility by membrane tension. *Trends Cell Biol.* 6:85–89.

Sheetz, M. P., D. B. Wayne, and A. L. Pearlman. 1992. Extension of filipodia by motor-dependent actin assembly. *Cell Motil. Cytoskel.* 22: 160.

Shen, Y., C. R. Safinya, K. S. Liang, A. F. Ruppert, and K. J. Rothschild. 1993. Stabilization of the membrane protein bacteriorhodopsin to 140°C in two-dimensional films. *Nature.* 366:48–50.

Simson, R., B. Yang, S. E. Moore, P. Doherty, F. S. Walsh, and K. A. Jacobson. 1998. Structural mosaicism on the submicron scale in the plasma membrane. *Biophys. J.* 74:297–308.

Thoumine, O., and A. Ott. 1997. Time scale dependent viscoelastic and contractile regimes in fibroblasts probed by microplate manipulation. *J. Cell Sci.* 110:2109–2116.

Turner, M. S., and P. Sens. 1997. Interactions between particulate inclusions in a smectic-A liquid crystal. *Phys. Rev. E.* 55:1275–1278.

Turner, M. S., and P. Sens. 1998. A multipole expansion for inclusions in a lamellar phase. *Phys. Rev. E.* 57:823–828.